

# Yb<sub>3</sub>Pt<sub>4</sub>: A New Route to Quantum Criticality

M. C. Bennett,<sup>1,2</sup> D. A. Sokolov,<sup>1,3</sup> M. S. Kim,<sup>1,3</sup> Y. Janssen,<sup>3</sup> Yuen Yiu,<sup>1,2</sup> W. J. Gannon,<sup>1</sup> and M. C. Aronson<sup>1,2,3</sup>

<sup>1</sup> *Department of Physics, University of Michigan, Ann Arbor, MI 48109-1120*

<sup>2</sup> *Department of Physics and Astronomy, Stony Brook University, Stony Brook, NY 11974 and*

<sup>3</sup> *Brookhaven National Laboratory, Upton, NY 11973*

(Dated: October 26, 2018)

We have studied the evolution of the weakly first order antiferromagnetic transition in heavy fermion Yb<sub>3</sub>Pt<sub>4</sub> using a combination of specific heat, magnetic susceptibility, and electrical resistivity experiments. We show that magnetic fields suppress the Neel temperature, as well as the specific heat jump, the latent heat, and the entropy of the transition, driving a critical endpoint at 1.2 K and 1.5 T. At higher fields, the antiferromagnetic transition becomes second order, and this line of transitions in turn terminates at a quantum critical point at 1.62 T. Both the ordered and high field paramagnetic states are Fermi liquids at low temperature, although the former has a much larger magnetic susceptibility and stronger quasiparticle scattering. Unlike previously studied quantum critical systems, the quasiparticle mass in Yb<sub>3</sub>Pt<sub>4</sub> does not diverge at the quantum critical point, implying that here the quasiparticle interactions drive the zero temperature transition. The Fermi liquid parameters are nearly field-independent in the ordered state, indicating that the fluctuations never become fully critical, as their divergences are interrupted by the first order antiferromagnetic transition.

PACS numbers: 75.30.Mb, 75.20.Hr, 71.27.+a

Quantum critical points (QCPs) are increasingly recognized [1] as organizing features of the phase diagram of strongly interacting electronic systems, from heavy electrons, [2, 3, 4] to complex oxides, [5, 6] and low dimensional conductors. [7] Since the QCP is a T=0 phase transition driven not by reduced temperature, but by varying parameters such as pressure or magnetic field, it is heralded by unusual non-Fermi liquid temperature dependences in measured quantities such as the electrical resistivity  $\rho$ , magnetic susceptibility  $\chi$ , and specific heat  $C$  [2, 3] which derive from quantum critical phenomena. [8] It is believed that the associated quantum critical fluctuations are crucial for stabilizing unconventional electronic states near QCPs, such as magnetically mediated superconductivity [9, 10] and electron nematic phases [11].

So far, magnetic phase diagrams hosting QCPs are found to fall into two distinct classes. Itinerant ferromagnets have been carefully studied, and in the cleanest systems the very lowest temperature phase transitions are first order, [12, 13] in agreement with theoretical expectations. [14] The implication is that the fluctuations near the quantum phase transition may not actually be fully critical, i.e. infinite in range and lifetime. In contrast, there are many examples among the heavy electron compounds of quantum critical antiferromagnets, where the Neel temperature can be driven to zero by an external parameter such as pressure or magnetic field. [15, 16, 17, 18] The success here of scaling analyses, particularly of neutron scattering data, [19, 20, 21] provides direct evidence for the dominance of quantum critical fluctuations in these compounds. While it is possible that closer scrutiny in cleaner systems will reveal as-yet hidden first order character, at present there are no known exceptions to the current theoretical and experimental consensus that all T=0 antiferromagnets are

second order, i.e. genuinely quantum critical.

The experimental record is clear that in these quantum critical antiferromagnets, the magnetic state emerges at T=0 from a Fermi liquid state, where the quasiparticle mass diverges as the tuning variable approaches its critical value [22, 23, 24, 25]. In some cases, this implied electronic localization is reflected in a discontinuous change in the Fermi surface volume at the QCP. [26, 27] We stress that much of this understanding has been gleaned from experimental and theoretical studies of antiferromagnets which are truly quantum critical, and that a very different development of the electronic structure may be possible in antiferromagnets where fluctuations play a less decisive role. Careful studies of the behaviors found in different parts of the phase diagram generated by tuning a first order antiferromagnetic transition are consequently very important, but only recently has a suitable experimental system been discovered.

We have recently reported that Yb<sub>3</sub>Pt<sub>4</sub> undergoes a weakly first order transition into an antiferromagnetic state with a Neel temperature  $T_N=2.4$  K, which is also a Fermi liquid. [28] Magnetic order develops from a simple paramagnetic state where the magnetic susceptibility obeys a Curie law, indicating that the Yb f-electrons are excluded from the Fermi surface for  $T \geq T_N$ . The crystal field scheme deduced from specific heat measurements reveals a well isolated magnetic doublet ground state, and the entropy associated with magnetic order is  $\sim 0.8 R \ln 2$ . We present here detailed measurements of the specific heat  $C$ , ac and dc magnetic susceptibility  $\chi$ , and electrical resistivity  $\rho$  using magnetic fields to tune the stability of antiferromagnetic order. The phase diagram revealed by these measurements is very different from any reported previously, with a line of first order transitions terminating at a critical endpoint, from which a line of second order transitions continues to a QCP. At low tem-

peratures, both the antiferromagnet and paramagnet are Fermi liquids, which evolve very differently as the QCP is approached.

Measurements of the specific heat  $C$  provide the first indication that magnetic fields oriented along the  $a$ -axis tune criticality in  $\text{Yb}_3\text{Pt}_4$ . Fig.1a shows that at every field  $C$  is well described by the sum of an electronic term  $\gamma T$ , a field independent phonon contribution  $\beta T^3$ , a broad Schottky contribution  $C_{Sch}$ , and a residual magnetic and electronic contribution  $C_M$  (Fig.1b), in which the onset of antiferromagnetic order at  $T_N$  is marked by a step-like anomaly  $\Delta C(T_N)$ . Magnetic fields reduce  $T_N$  (Fig.2a), while  $\Delta C$  and the latent heat  $L$  of the transition are suppressed continuously to zero at 1.5 T (Fig.2b). The broad Schottky peak traverses our temperature window with increasing field, and the inset of Fig.1a shows the related Zeeman splitting  $\Delta$  of the ground doublet. We have plotted the entropy  $S$  associated with  $C_M$  in Fig.2b, which is reduced from its zero field value of  $\sim 0.8 R \ln 2$  to zero in a field of 1.5 T. Taken together, these data show that all thermodynamic signatures of the first order transition vanish simultaneously at 1.5 T, although  $T_N$  remains nonzero. We conclude that the line of first order antiferromagnetic transitions which originates from the zero field value of 2.4 K extends to a critical endpoint at 1.2 K and 1.5 T ( $H \parallel a$ ). Similar measurements reveal that the critical endpoint occurs at 1.2 K and 3.5 T when  $H \parallel c$ .

The first order phase line  $T_N(H)$  is also evident in other measurements. While the magnetization  $M$  is continuous at  $T_N(H)$ , its field and temperature derivatives are discontinuous. The temperature dependence of the real part of the ac susceptibility  $\chi'$  is plotted for different fixed fields in Fig.1c. In low fields, an antiferromagnetic cusp is observed at the Neel temperature  $T_N$ . With increased field, steplike discontinuities in  $\chi'$  and also in  $dM/dT$  (not shown here) occur at the same ordering temperatures found in  $C$  (Fig.2a), in both cases becoming stronger as the field approaches the critical endpoint at 1.5 T. Fig.1c shows that these manifestations of the phase transition in  $\chi'$  are superposed on a field and temperature dependent background, which is Curie-like at low fields, and then develops a broad maximum which moves to higher temperatures with increasing field. In every field, Curie-law behavior is regained at high temperatures. The inset of Fig.1c shows a calculation of  $\chi(T)$ , assuming a two level system with different values of the doublet splitting  $\Delta$  which qualitatively reproduces this behavior.

It is of great interest to determine whether the first order phase line extends beyond the critical endpoint as one or more lines of second order phase transitions, or simply gives way to a coexistence regime. Accordingly,  $C(H)$  is plotted at different fixed temperatures in Fig. 1d. For temperatures which are larger than the 1.2 K critical endpoint ( $T_{CEP}$ ), a step is observed in  $C(H)$ , reminiscent of the step in  $C(T)$  shown in Fig.1b. For  $T \leq T_{CEP}$ , the step becomes a lambda-like anomaly, as expected for a second order phase transition. This peak in  $C(H)$  moves

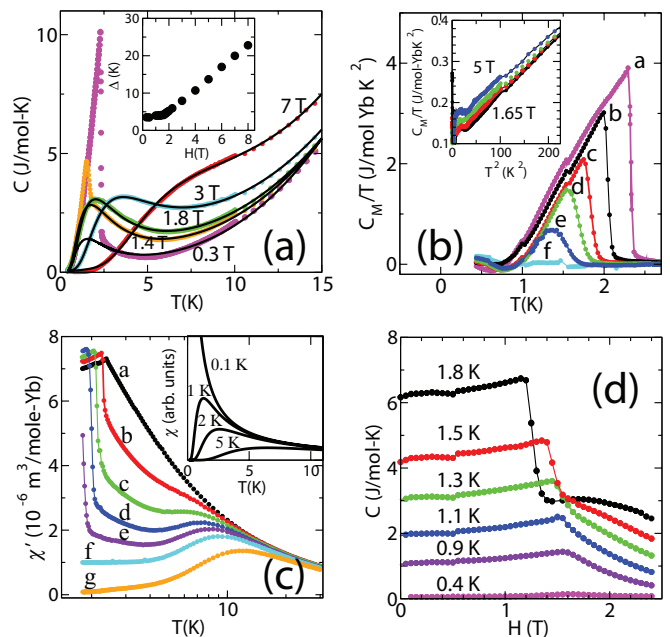


FIG. 1: (a) The specific heat  $C$  of  $\text{Yb}_3\text{Pt}_4$  measured in magnetic fields  $H \parallel a$ . Solid lines are fits to  $C(T) = C_{Sch} + \gamma T + \beta T^3$ . Inset: The splitting  $\Delta$  of the ground state doublet in field. (b)  $C_M/T = (C - C_{Schottky})/T$  in different fields (a=0.3 T, b=1 T, c=1.25 T, d=1.37 T, e=1.5 T, f=1.65 T). Inset:  $C_M/T$  plotted as a function of  $T^2$  for  $H=1.65$  T, 2.25 T, 3 T, and 5 T. The steps near 10 K reflect a systematic error in the PPMS temperature calibrations. (c) The real part of the ac susceptibility  $\chi'$  for different fields  $H \parallel a$  (a=0.1 T, b=0.6 T, c=0.9 T, d=1.1 T, e=1.3 T, f=1.6 T, g=2.5 T). Inset: Calculated  $\chi(T)$  for different values of  $\Delta$ , the splitting of an isolated  $\text{Yb}^{3+}$  doublet. (d) The field dependence of the specific heat  $C$  ( $H \parallel a$ ) at fixed temperatures 0.4 K - 1.8 K.

to slightly higher fields and is reduced in amplitude as the temperature is reduced. The peaks in  $C(H)$  shown in Fig.1d trace out a line of second order transitions which terminates at a zero temperature QCP with a critical field  $H_{QCP}$  of  $\sim 1.6$  T (Fig.2a). Further evidence for a second order line emanating from the critical endpoint comes from the field dependence of the electrical resistivity  $\rho(H)$ , shown Fig.3a. For scans across the first order phase line ( $T \geq 1.2$  K),  $\rho$  is continuous, like  $M$ , but  $d\rho/dH$  is discontinuous, like  $\chi = dM/dH$ . For lower temperatures ( $T \leq 1.2$  K) where we are scanning across the second order phase line,  $\rho(H)$  develops a cusp, signalling an incipient divergence of the magnetization. Taken together, the first and second order lines are well described by the expression  $T_N \propto (H - H_{QCP})^{0.28 \pm 0.03}$  with  $H_{QCP} = 1.62$  T. We note that this critical exponent is much smaller than  $2/3$ , the value expected for a mean field quantum critical antiferromagnet, [8] and does not reproduce the quasi-linear suppression of  $T_N$  found in other quantum critical antiferromagnets. [15, 16]

Our measurements indicate that both the antiferromagnetic state and the high field paramagnetic state are

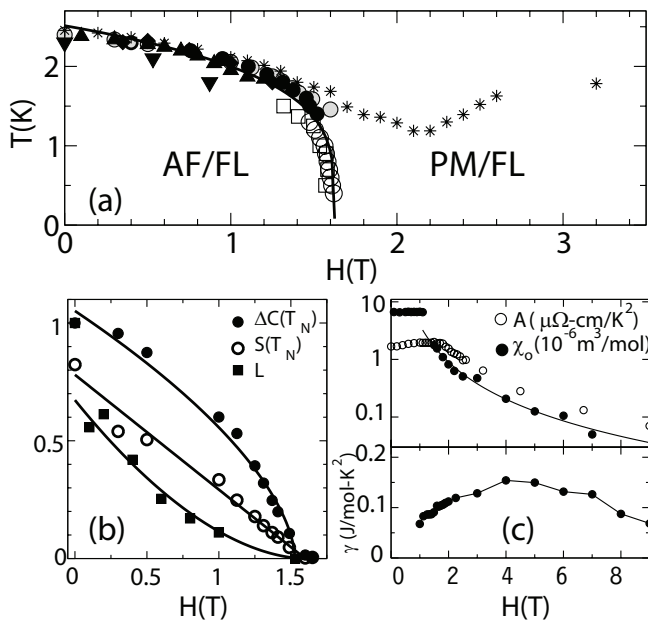


FIG. 2: (a) The magnetic phase diagram of  $\text{Yb}_3\text{Pt}_4$  for  $H\parallel a$  taken from temperature sweeps of  $\chi$  ( $\blacktriangle$ ),  $dM/dT$  ( $\blacklozenge$ ),  $C(T)$  (gray circles) and field sweeps of  $C(H)$  (1<sup>st</sup> order:  $\bullet$ , 2<sup>d</sup> order:  $\circ$ ) and  $\rho(H)$  (1<sup>st</sup> order:  $\blacktriangledown$ , 2<sup>d</sup> order:  $\square$ ).  $T_{FL}$  (\*) is the limit of  $\Delta\rho \sim T^2$ . The first and second order lines are jointly fit by  $T_N \sim (H-1.62 \text{ T})^{0.28}$  (solid line). (b)  $\Delta C(T_N)$  (normalized to zero field value 8.82 J/mol-K, filled circles), entropy  $S(T_N)$  (units of  $\text{Rln}2$ , open circles), latent heat  $L$  (normalized to zero field value 0.09 J/mol-Yb, filled squares) Lines are guides for the eye. (c) Field dependencies of the Fermi liquid parameters  $A$ ,  $\chi_0$ , and  $\gamma$ , defined in the text. Solid line for  $\chi_0 \propto 1/H^3$ , solid line for  $\gamma$  is guide for eye.

Fermi liquids. We have tracked their development by measuring the temperature dependence of  $\Delta\rho/\rho = (\rho(T) - \rho(T=0))/\rho(T=0)$  in fixed fields both above and below the quantum critical field  $H_{QCP} = 1.62 \text{ T}$  (Fig.3b).  $\Delta\rho = A(H)T^2$  below an effective Fermi temperature  $T_{FL}$  which is indistinguishable from  $T_N$  for fields  $H \leq H_{QCP}$  (Fig. 2a). Long lived and long ranged critical fluctuations generally suppress Fermi liquid behavior near the onset of order, so the resilience of the antiferromagnetic Fermi liquid in  $\text{Yb}_3\text{Pt}_4$  is remarkable, perhaps reflecting a general weakness of critical fluctuations near a first order transition. The quadratic temperature dependence for  $\Delta\rho$  extends well into the paramagnetic phase  $H \geq H_{QCP}$ , with  $T_{FL}$  reaching its minimum value near the critical endpoint before increasing again with increasing magnetic fields. Fig.3b also shows that the resistivity coefficient  $A(H)$  is almost field independent within the antiferromagnetic phase  $H \leq H_{QCP}$ , and then drops rapidly at larger fields. These observations are quantified in Fig. 2c, where  $A$  decreases by a factor of  $\sim 30$  from its value in the antiferromagnetic low field phase to its value in 9 T.

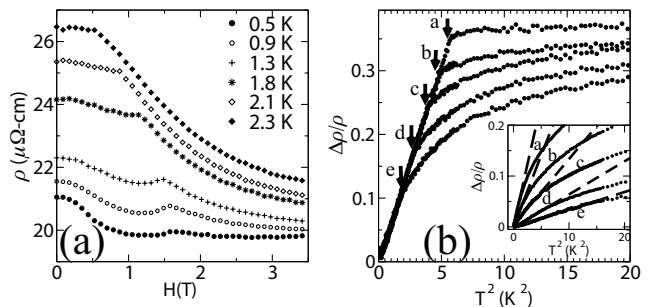


FIG. 3: (a) The field dependence of the electrical resistivity  $\rho$  for fixed temperatures 0.5 K - 2.3 K ( $H\parallel a$ ). (b)  $\Delta\rho/\rho = \rho(T) - \rho_0/\rho_0$  is linear in  $T^2$  up to  $T_{FL} = T_N$  (marked by arrows). (a,b,c,d,e correspond to 0, 0.8 T, 1.2 T, 1.5 T, 1.8 T). Inset: same, but with  $H \geq H_{QCP} = 1.62 \text{ T}$ . (a,b,c,d,e correspond to 2.3 T, 3.2 T, 4.5 T, 6.7 T, 9 T). Dashed lines are linear fits.

The magnetic susceptibility also suggests that the ordered state is a Fermi liquid. Fig.1c shows that  $\chi/T$  for  $T \leq T_N$  consists of a large and temperature independent term  $\chi_0$  and a much weaker temperature dependent contribution. No trace is found in the antiferromagnetic state of the local moment behavior found in the susceptibility for  $T \geq T_N$ , suggesting that here the f-electron has been absorbed into the Fermi surface.  $\chi_0$  is plotted as a function of field in Fig.2c. While slight variations in field alignment are likely responsible for the slightly different values of  $H_{QCP}$  found in the different measurements,  $\chi_0$ , like  $A$ , is nearly field independent in the ordered state, but falls off dramatically in the paramagnetic state ( $H \geq H_{QCP}$ ).

The interpretation of the specific heat data is more complex. The convolution of the Schottky and ordering peaks makes it impossible to unambiguously isolate the Fermi liquid part of the specific heat at the lowest fields. We limit our analysis to fields larger than 1.4 T, where the inset to Fig.1b confirms there is a linear contribution to  $C$  with a magnitude  $\gamma$  which increases from  $\sim 60 \text{ mJ/mol-K}^2$  at 1.4 T to a maximum value of  $160 \text{ mJ/mol-K}^2$  at 5 T, before falling off at higher fields (Fig.2c).

The field evolution of the Fermi liquid parameters  $A$ ,  $\chi_0$ , and  $\gamma$  reveals an unusual sequence of events which accompany the onset of antiferromagnetic order in  $\text{Yb}_3\text{Pt}_4$ . Unlike other systems where the destruction of the quasiparticles at the QCP is mirrored in the divergence of the quasiparticle mass, in  $\text{Yb}_3\text{Pt}_4$   $\gamma$  is only weakly field dependent. Since  $\chi_0 \propto m^*/m (1/(1+F_0^a))$ , we conclude that in the absence of a diverging quasiparticle mass enhancement  $m^*/m$ , the field dependence of  $\chi_0$  must be dominated in  $\text{Yb}_3\text{Pt}_4$  by that of  $(1/(1+F_0^a))$ . Fig. 4 shows that  $\chi_0/\gamma$  increases from a value of  $5 \times 10^{-8} \text{ m}^3\text{K}^2/\text{mJ}$  at 9 T, typical of other heavy electron compounds [29], to its final value of  $2 \times 10^{-4} \text{ m}^3\text{K}^2/\text{mJ}$  at  $H_{QCP}$ , corresponding to a divergence  $\chi_0/\gamma \propto 1/(1+F_0^a) \sim H^{-3 \pm 0.2}$ . We stress that this field dependence is not well described by  $1/(H-$

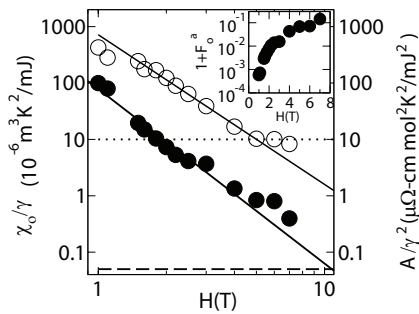


FIG. 4: The field dependencies of the Sommerfeld-Wilson ratio  $\chi_0/\gamma$  (filled circles, left axis) and the Kadowaki-Woods ratio  $A/\gamma^2$  (open circles, right axis). Solid lines are power law fits, described in the text. Dotted line:  $A/\gamma^2=10\mu\Omega\text{-cm mol}^2\text{K}^2/\text{J}^2$ , dashed line:  $\chi_0/\gamma=5\times 10^{-8}\text{m}^3\text{K}^2/\text{mJ}$ . Inset: The field dependence of  $1+F_0^a$ .

$H^*)^n$  for any nonzero  $H^*$ , or for any  $n$ .  $1/1+F_0^a$  can be isolated using  $R_W=\pi^2k_B^2\chi_0/(\mu_0\mu_{eff}\gamma)=1/(1+F_0^a)$  (Fig. 4, inset).  $1+F_0^a$  approaches zero, implying that enhanced long-range interactions among the quasiparticles may drive the  $T=0$  phase transition, much as in a Stoner ferromagnet, or in  $^3\text{He}$  itself. A matching divergence in the Kadowaki-Woods ratio  $A/\gamma^2 \propto 1/H^{2.6\pm 0.2}$  (Fig. 4) reveals that the normal heavy electron behavior  $A/\gamma^2=10\mu\Omega\text{-cm mol}^2\text{K}^2/\text{J}^2$  found at large fields [30] is supplanted by a sixty-fold increase in the quasiparticle - quasiparticle scattering. If the diverging exchange field were primarily ferromagnetic, as implied by  $F_0^a \rightarrow -1$  (Fig. 4, inset), we would expect forward scattering to dominate the transport, with  $A(H)\propto \chi^2$ . [31, 32] Instead we have  $A(H)\propto \chi$ , suggesting that quasiparticle interactions with nonzero wave vector are likely also strengthening

on the approach to the antiferromagnetic state. Finally, the saturation of  $A$  and  $\chi_0$  in the ordered state with  $H\leq H_{QCP}$  signals that the first order onset of long range antiferromagnetic order cuts off further development of these quasiparticle correlations.

In conclusion, our data indicate that  $\text{Yb}_3\text{Pt}_4$  is unique among quantum critical systems studied so far. It has an unusual phase diagram, where a weakly first order phase line terminates at a critical endpoint, and is continued along a second order phase line to a QCP, where the critical phenomena are emphatically not mean-field like. The zero temperature magnetic susceptibility increases rapidly as the field approaches this quantum critical field, but this divergence is controlled by a fixed point at zero field which is prematurely cut off by magnetic order, and no evidence is found for strong fluctuations associated with the QCP. Fermi liquid behavior is found on both sides of this field driven QCP, although the antiferromagnetically ordered Fermi liquid at low fields is more strongly interacting than the paramagnetic Fermi liquid above the quantum critical field. Unlike previously studied systems, there is no divergence of the quasiparticle mass at the quantum critical field, although the interactions among the quasiparticles strengthen dramatically, suggesting that they interact with each other in a medium which becomes progressively more susceptible, eventually culminating in magnetic order. This scenario is unique among the heavy electron compounds studied so far, and demonstrates that  $\text{Yb}_3\text{Pt}_4$  represents a new route to quantum criticality.

The authors acknowledge useful conversations with C. Varma, Q. Si, P. Coleman, E. Abrahams, G. Zwircknagl, and V. Zlatić. Work at Stony Brook University and the University of Michigan was supported by the National Science Foundation under grant NSF-DMR-0405961.

- 
- [1] P. Coleman and A. J. Schofield, *Nature* **433**, 226 (2005).
  - [2] G. R. Stewart, *Rev. Mod. Phys.* **73**, 797(2001).
  - [3] H. v. Lohneysen, et al., *Rev. Mod. Phys.* **79**, 1015 (2007).
  - [4] P. Gegenwart, et al., *Nature Physics* **4**, 186 (2008).
  - [5] R. B. Laughlin, *Adv. Phys.* **47**, 943(1998).
  - [6] C. M. Varma, et al., *Phys. Rev. Lett.* **63**,1996(1999).
  - [7] D. Jaccard, et al., *J. Phys.: Cond. Matter* **13**, L89 (2001).
  - [8] A. J. Millis, *Phys. Rev. B* **48**, 7183 (1993).
  - [9] N. D. Mathur, et al., *Nature* **394**, 39(1998).
  - [10] S. Saxena, et al., *Nature* **406**, 587 (2000).
  - [11] R. A. Borzi, et al., *Science* **315**, 214 (2007).
  - [12] C. Pfleiderer, *J. Phys. : Cond. Matter* **17**, S987 (2005).
  - [13] Y. J. Uemura, et al. *Nature Physics* **3**, 29 (2007).
  - [14] D. Belitz, et al., *Rev. Mod. Phys.* **77**, 579 (2005).
  - [15] S. R. Julian, et al., *J. Phys.: Condensed Matter* **8**, 9675 (1996).
  - [16] H. von Lohneysen, *J. Phys.: Condensed Matter* **8**, 9689 (1996).
  - [17] P. Gegenwart, et al., *J. Low. Temp. Phys.* **133**, 3 (2003).
  - [18] S. L. Bud'ko, et al., *Phys. Rev. B* **69**, 014415 (2004).
  - [19] M. C. Aronson, et al., *Phys. Rev. Lett.* **75**, 725 (1995).
  - [20] M. C. Aronson, et al., *Phys. Rev. Lett.* **87**,197205 (2001).
  - [21] A. Schroder et al, *Nature* **407**, 351 (2000).
  - [22] F. Steglich, et al., *Physica B* **237**, 192 (1997).
  - [23] P. Gegenwart, et al., *Acta Phys. Polonica* **34B**,323(2003).
  - [24] S. Nakamura, et al., *Phys. Rev. Lett.* **97**, 237204 (2006).
  - [25] P. Coleman, et al., *J. Phys.: Condens. Matt.***13**, R723 (2001).
  - [26] H. Shishido, et al., *J. Phys. Soc. Japan* **74**, 1102 (2005).
  - [27] S. Paschen, et al., *Nature* **432**, 881(2004).
  - [28] M. C. Bennett, et al., arXiv:0806.1943v1.
  - [29] Z. Fisk, et al, *Japanese Journal of Applied Physics* **26** Suppl. 3, 1882 (1987).
  - [30] N. Tsujii, et al, *J. Phys.: Cond. Matt.* **15**, 1993 (2003).
  - [31] K. S. Dy and C. J. Pethick, *Phys. Rev.* **185**, 373 (1969).
  - [32] G. Zwircknagl, *Adv. Phys.* **41**, 203 (1992).